

$\pi$  back-donation. The value of  $\Delta E_{\text{Pt-L}}/(\Delta E_{\text{Pt-P}} + \Delta E_{\text{Pt-P}})$  represents which of the Pt-L or Pt-P bond is altered largely by the ligand orientation, where  $\Delta E_{\text{Pt-L}}$  is the difference in the  $E_{\text{Pt-L}}$  value (see eq 2 for  $E_{\text{Pt-L}}$ ) between structures A and B. As shown in Figure 6, a linear relation is obtained between the  $q(\pi^*)$  value and  $\Delta E_{\text{Pt-L}}/(\Delta E_{\text{Pt-P}} + \Delta E_{\text{Pt-P}})$ ,<sup>19</sup> where the  $\Delta E_{\text{Pt-L}}/(\Delta E_{\text{Pt-P}} + \Delta E_{\text{Pt-P}})$  value becomes smaller with an increase in the  $q(\pi^*)$  value. When the L ligand is a sufficiently strong Lewis acid such as the dioxygen ligand (i.e., the  $q(\pi^*)$  is large), the  $d\pi-\pi^*$  interaction is strong in any orientation of the L ligand. Thus, the Pt-L bond strength hardly depends on the orientation, while the Pt-PH<sub>3</sub> bond strength is altered by the orientation. In such a case, the  $\Delta E_{\text{Pt-L}}/(\Delta E_{\text{Pt-P}} + \Delta E_{\text{Pt-P}})$  value becomes small, as shown in Figure 6, and the structure of Pt(PH<sub>3</sub>)<sub>2</sub>L is arranged to strengthen the Pt-L bond. On the other hand, in cases such as ethylene, acetylene, and carbon disulfide, where the L ligand has relatively weak Lewis acidity (i.e., the  $q(\pi^*)$  value is small), the  $d\pi-\pi^*$  interaction also depends on the orientation. Consequently, the strength of both the Pt-L and Pt-PH<sub>3</sub> bonds is altered by the orientation. In such a case, the  $\Delta E_{\text{Pt-L}}/(\Delta E_{\text{Pt-P}} + \Delta E_{\text{Pt-P}})$  value becomes large relative to that in the case of the dioxygen ligand, and the stability of structure A attributes to the strengthening of both the Pt-L and Pt-PH<sub>3</sub> bonds. In conclusion, a decrease in the Lewis acidity of the L ligand makes the value of  $\Delta E_{\text{Pt-L}}/(\Delta E_{\text{Pt-P}} + \Delta E_{\text{Pt-P}})$  large, as shown in Figure 6, and in such a case both the Pt-L and Pt-PH<sub>3</sub> bonds play a role in determining the structure of Pt(PH<sub>3</sub>)<sub>2</sub>L.

In this work, the stereochemistry of Pt(PH<sub>3</sub>)<sub>2</sub>L (L = C<sub>2</sub>H<sub>4</sub>, C<sub>2</sub>H<sub>2</sub>, or CS<sub>2</sub>) is successfully explained by considering the interaction shown in Scheme Ia. It is shown that the main factor which stabilizes structure A is different for the complexes examined here and the dioxygen complex and that this difference is due to the difference in their Lewis acidity. The importance of the interaction shown in Scheme Ia is supported by frontier orbital theory.

**Acknowledgment.** MO calculations were performed with the Facom M-190 Computer at the Data Processing Center of Kyushu University. This work was supported partially

by the grant of the Ministry of Education (No. 435045).

## References and Notes

- (1) (a) Herberhold, M. "Metal  $\pi$ -Complexes"; Elsevier: Amsterdam, 1972; Vol. II. (b) Hartly, F. R. "The Chemistry of Platinum and Palladium"; Applied Science Publishers: London, 1973. (c) Taqui Khan, M. M.; Martell, A. E. "Homogeneous Catalysis by Metal Complexes"; Academic Press: New York, 1974. (d) Jolly, P. W.; Wilke, G. "The Organic Chemistry of Nickel"; Academic Press: New York, 1974 and 1975; Vol. I and II.
- (2) For example, Norman, J. G., Jr. *Inorg. Chem.* **1977**, *16*, 1328.
- (3) Sakaki, S.; Hori, K.; Ohyoshi, A. *Inorg. Chem.* **1978**, *17*, 3138.
- (4) Cook, C. D.; Wan, K. Y.; Gellus, U.; Hamrin, K.; Johansson, G.; Olsson, E.; Siegbahn, H.; Nordling, C.; Siegbahn, K. *J. Am. Chem. Soc.* **1971**, *93*, 1904.
- (5) (a) Panattoni, C.; Bombieri, G.; Belluco, U.; Baddley, W. H. *J. Am. Chem. Soc.* **1968**, *90*, 798. (b) Francis, J. N.; McAdam, A.; Ibers, J. A. *J. Organomet. Chem.* **1971**, *29*, 131 and 149. (c) Barahan, J. M.; McGinnety, J. A. *J. Am. Chem. Soc.* **1975**, *97*, 4232. (d) Cheng, P.-T.; Cook, C. D.; Nyburg, S. C.; Wan, K. Y. *Inorg. Chem.* **1971**, *10*, 2210.
- (6) Gianville, I. O.; Stewart, J. M.; Grim, S. O. *J. Organomet. Chem.* **1967**, *7*, 9.
- (7) Mason, R.; Rae, A. I. M. *J. Chem. Soc. A* **1970**, 1767.
- (8) Cheng, P.-T.; Cook, C. D.; Nyburg, S. C.; Wan, K. Y. *Can. J. Chem.* **1971**, *49*, 3772. Kashiwagi, T.; Yasuoka, N.; Kasai, N.; Kakudo, M.; Takahashi, S.; Hagihara, N. *Chem. Commun.* **1969**, 743.
- (9) Sakaki, S.; Hagihara, N.; Iwasaki, N.; Ohyoshi, A. *Bull. Chem. Soc. Jpn.* **1977**, *50*, 14.
- (10) Sakaki, S.; Kudou, N.; Ohyoshi, A. *Inorg. Chem.* **1977**, *16*, 202.
- (11) Pople, J. A.; Segal, G. A. *J. Chem. Phys.* **1966**, *44*, 3289.
- (12) Gordon, M. S. *J. Am. Chem. Soc.* **1969**, *91*, 3122. Ehrenson, S.; Seltzer, S. *Theor. Chim. Acta* **1971**, *20*, 17.
- (13) Fujimoto, H.; Kato, S.; Yamabe, S.; Fukui, K. *J. Chem. Phys.* **1974**, *60*, 572.
- (14) ZDO approximation was introduced, when using eq 4 and 5 of ref 13.
- (15) Strictly speaking, the strength of the Pt-L interaction also depends on the product of the  $p_x$  orbital's LCAO coefficient and the resonance integral between the coordinating atom and the platinum(0). This quantity of the  $\pi$  MO is almost the same degree as that of the  $\pi'$  MO. Therefore, the difference in the donating ability between the  $\pi$  and  $\pi'$  MOs is mainly due to the difference in the orbital energies between these two MOs.
- (16) For example, Fukui, K.; Fujimoto, H. *Bull. Chem. Soc. Jpn.* **1969**, *42*, 3399.
- (17) The HOMO,  $6a_1$ , cannot form any bonding interaction with the  $\pi^*$  orbital of the L ligand, and the second HOMO lies in almost the same energy level as the HOMO. The HOMO was excluded from the discussion.
- (18) Fukui, K.; Inagaki, S. *J. Am. Chem. Soc.* **1975**, *97*, 4445.
- (19) The linear relation is not necessarily obtained. It is expected that the  $\Delta E_{\text{Pt-L}}/(\Delta E_{\text{Pt-P}} + \Delta E_{\text{Pt-P}})$  value increases with a decrease in the L ligand Lewis acidity, in general.

## Møller-Plesset Study of the H<sub>4</sub>CO Potential Energy Surface

L. B. Harding,<sup>1a</sup> H. B. Schlegel,<sup>1b</sup> R. Krishnan, and J. A. Pople\*

Department of Chemistry, Carnegie-Mellon University, Pittsburgh, Pennsylvania 15213 (Received: June 26, 1980)

Ab initio second-, third-, and fourth-order, 6-31G\*\*, Møller-Plesset perturbation theory results are presented for eight minimum energy structures and six transition structures on the H<sub>4</sub>CO potential energy surface. The most accurate, 0 K calculated activation energies are as follows: H<sub>2</sub>CO  $\rightarrow$  H<sub>2</sub> + CO,  $E_a$  = 88.0 kcal/mol; H<sub>2</sub>CO  $\rightarrow$  HCOH (trans),  $E_a$  = 86.2 kcal/mol; HCOH (trans)  $\rightarrow$  HCOH (cis),  $E_a$  = 28.6 kcal/mol; H<sub>2</sub> + H<sub>2</sub>CO  $\rightarrow$  H<sub>3</sub>COH,  $E_a$  = 80.1 kcal/mol; H<sub>2</sub> + HCOH (trans)  $\rightarrow$  H<sub>3</sub>COH,  $E_a$  = 19.1 kcal/mol; CH<sub>2</sub>(<sup>1</sup>A<sub>1</sub>) + H<sub>2</sub>O  $\rightarrow$  H<sub>3</sub>COH,  $E_a$  = 0.0 kcal/mol. These results are compared both to previously reported CI studies and to experimental results.

## Introduction

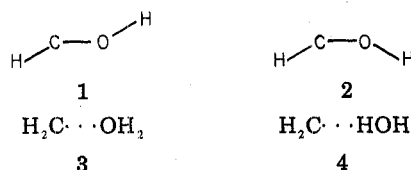
It is now well established that electron correlation effects may be of importance in studying even qualitative features of reaction potential surfaces.<sup>2</sup> Correlation is known to make a large contribution to covalent bond energies. Indeed the neglect of correlation can lead to errors in excess

of 50 kcal/mol in calculated bond energies.<sup>3</sup> It should not be surprising then to find that activation energies, usually involving transition structures with partially broken bonds, are also very sensitive to correlation effects.<sup>4</sup>

In a series of preceding papers a number of computationally efficient methods of incorporating electron cor-

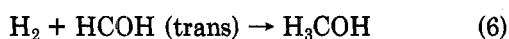
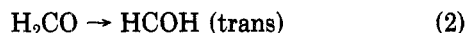
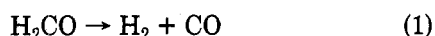
relation into ab initio calculations were presented.<sup>4-6</sup> The resulting theoretical models, *n*th order Møller-Plesset (MP*n*) perturbation theory, have been applied to the determination of a large number of equilibrium geometries<sup>7</sup> and to an examination of several simple molecular rearrangements, 1,2 hydrogen migrations.<sup>4</sup> In this paper we present the results of Møller-Plesset calculations on a more complex chemical system, portions of which have been well characterized with both experimental and theoretical methods and other portions of which are as yet poorly understood.

The system chosen is the H<sub>4</sub>CO potential energy surface. The minimum energy structures considered here include molecular hydrogen, carbon monoxide, formaldehyde, methanol, and the following less stable structures:



Of the later four structures, extensive ab initio calculations<sup>8-10</sup> have been reported only for 1 and 2. The most recent study, by Goddard and Schaefer (GS),<sup>9</sup> consisted of double zeta plus polarization configuration interaction (CI) calculations and provides an excellent comparison of conventional CI techniques to the MP calculations presented here.

In addition to the above minimum energy structures, transition states for the following reactions have also been examined:



Of these reactions only reaction 1 has been well characterized experimentally.<sup>11</sup> Molecular photodissociation is found to occur at energies near the excited singlet (*S*<sub>1</sub>) origin (80.6 kcal/mol).<sup>12</sup> At higher energies<sup>13</sup> a competing radical dissociation process leading to atomic hydrogen and formyl radicals also occurs. The thermodynamic and photodissociation thresholds for the latter are both in the range of 85–87 kcal/mol.<sup>14,15</sup>

Reactions 1–3 have been the focus of several theoretical studies, the most extensive of which has been recently reported by Goddard and Schaefer.<sup>9</sup> Using a “double zeta” plus polarization function basis and all single- and double-substitution CI calculations, with an approximate correction for higher order excitations (quadruples), they find activation energies for reactions 1–3 of 93.6 (87), 88.8 (89.3), and ~28 kcal/mol, respectively. (For the first two, zero-point corrections were also calculated, and the resulting zero-point-corrected activation energies are given in parentheses.) GS further suggest that the lower observed threshold for reaction 1, 80.6 vs. 87 kcal/mol, may be the result of tunneling. Indeed Miller<sup>16</sup> has reported a calculation on the tunneling correction for this reaction rate using the transition-state vibrational frequencies reported by Goddard and Schaefer. He concludes that the rate of tunneling through a zero-point-corrected barrier of 87 kcal/mol is large enough to account for the observed

molecular products at 80.6 kcal/mol.

Much less information is currently available on reactions 4–6. To our knowledge no ab initio calculations including the effects of correlation have been reported for any of these three reactions. In addition, no experimental information on the rates, thresholds, or activation energies for these three processes is available. However these three are all excellent prototypes for large classes of common reactions. Reaction 4 is a classical 2 + 2 asymmetric addition, while reactions 5 and 6 are examples of carbene insertion reactions, one (reaction 5) involving an unsubstituted carbene and the second (reaction 6) a hydroxy-substituted carbene. Comparison then of the results for reaction 6 with a previous study of the H<sub>2</sub> + CH<sub>2</sub> insertion will provide information on the effect of substitution on carbene reactivity.

### Computational Methods

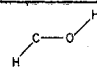
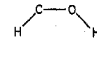
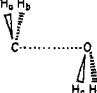
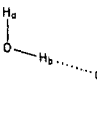
A number of theoretical models are employed in this work, the difference between these models being the flexibility of the basis sets and the level or order of perturbation theory used both in the geometry optimizations and for single-point studies at the calculated equilibrium or transition structures. The correlation technique used here is Møller-Plesset perturbation theory terminated at second (MP2), third (MP3), or fourth (MP4) order.<sup>5,6</sup> The fourth-order calculations are incomplete in the sense that the effect of triple excitations are neglected, only single, double, and quadruple excitations being included.<sup>6</sup> Except where noted, all of the calculations here employ the spin-restricted formalism (restricted Hartree-Fock, RHF, or restricted Møller-Plesset, RMP*n*) requiring that the *α* and *β* spatial orbitals be identical. The RMP calculations reported here are frozen core results, in which excitations out of the carbon and oxygen 1s orbitals are excluded. The computational details of these methods have been discussed elsewhere<sup>4-6</sup> and will not be presented here.

We report here two classes of theoretical models: one in which the perturbation theory calculations are carried out at the calculated HF equilibrium (or transition) structure and a second class in which the geometries are obtained with RMP2 optimizations. In both models the geometry optimizations were carried out by using the gradient method in which the first derivative of the energy with respect to the nuclear coordinates is calculated analytically at each point and the result used to determine the direction of steepest descent.<sup>17</sup>

The basis used in the geometry optimizations is the 6-31G\* polarization set.<sup>18</sup> At the calculated optimum geometries this basis was augmented by the addition of hydrogenic p-polarization functions (*α* = 1.10) forming what is termed the 6-31G\*\* basis.<sup>18</sup> Unless otherwise noted, all of the relative energies reported here were obtained with the 6-31G\*\* basis. In conclusion, we report studies using similar bases which might be useable in larger systems. These results, which are not vital to the present studies of H<sub>4</sub>CO, are placed in the Appendix.

Analytic second derivatives of the energy with respect to nuclear coordinates were calculated at the RHF/6-31G\* optimum geometries (using the 6-31G\* basis sets). The resulting force constants are then used to obtain harmonic vibrational frequencies and associated zero-point energies. For transition structures, of course, one frequency is imaginary, and this frequency is neglected in the zero-point summation. The computational details of the second-derivative calculations have been presented previously.<sup>17</sup> All calculations were carried out by using the GAUSSIAN 80/CMU program<sup>19</sup> on a Digital Equipment Corp. VAX 11/780 digital computer.

TABLE I: Calculated RHF and RMP2 (6-31G\*) Equilibrium Structures<sup>a</sup>

structure	geometry RHF/6-31G* (RMP2/6-31G*)
1. 	$R_{CO} = 1.300$ (1.323), $R_{CH} = 1.099$ (1.113), $R_{OH} = 0.951$ (0.978), $HCO \angle = 103.0$ (101.4), $HOH \angle = 109.4$ (107.2)
2. 	$R_{CO} = 1.298$ (1.317), $R_{CH} = 1.107$ (1.122), $R_{OH} = 0.953$ (0.985), $HCO \angle = 107.1$ (106.6), $HOH \angle = 116.1$ (115.5)
3. 	$R_{CO} = 2.138$ (1.805), $R_{CH} = 1.094$ (1.105), $R_{OH} = 0.949$ (0.976), $H_aCH_b \angle = 102.7$ (102.2), $H_cOH_d \angle = 105.0$ (103.4), $H_{ab}CO \angle = 88.9$ (96.0), $H_{cd}OC \angle = 102.5$ (101.4)
4. 	$R_{OH_a} = 0.947$ (0.968), $R_{OH_b} = 0.954$ (0.978), $R_{CH_b} = 2.274$ (2.153), $R_{CH_c} = 1.094$ (1.105), $R_{CH_d} = 1.093$ (1.105), $H_aOH_b \angle = 105.2$ (103.8), $OH_bC \angle = 179.1$ (177.4), $H_bCH_c \angle = 136.9$ (137.1), $H_bCH_d \angle = 118.8$ (119.3)

<sup>a</sup> Bond lengths are given in angstroms and  $H_{ab}XY$  denotes the angle between the  $H_aXH_b$  bisector and the  $XY$  bond.

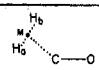
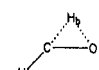
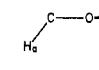
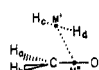
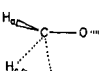
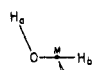
## Results and Discussion

**Comparison of RHF and RMP2 Geometries.** With the introduction of efficient gradient optimization techniques, it has become possible to optimize the geometries of large molecules by using large basis set HF calculations. The computational requirements of calculations employing correlated wave functions are, however, much more severe than those of HF theory. For this reason it is not yet practical to carry out complete geometry optimizations for large molecules with correlated wave functions, and it is therefore important to determine the magnitude of the error introduced through the use of less accurate HF geometries. In this section we compare the results of RHF and RMP2 geometry optimizations for the various  $H_2CO$  equilibrium and transition structures. As this surface includes examples of many different types of equilibrium species and reactions, we expect the conclusions reached here to be applicable to a large area of chemistry.

The structures resulting from RHF/6-31G\* and RMP2/6-31G\* optimizations are presented in Tables I and II. Those previously reported<sup>7</sup> (hydrogen, carbon monoxide, formaldehyde, and methanol equilibrium structure) are not repeated. For all of the RHF structures, the number of negative eigenvalues of the second-derivative matrix has been checked (zero for equilibrium structures and one for transition structures). However, this check was not carried out at the RMP2 level. The four equilibrium structures 1-4 (Table I) all have a plane of symmetry (point group  $C_s$ ). 5 and 6 are the transition structures for molecular dissociation (reaction 1) and 1,2 hydrogen shift (reaction 2). Both are planar. Structure 7 (nonplanar, point group  $C_1$ ) determines the barrier for internal rotation in hydroxycarbene. Structure 8 is the transition structure for 1,2 addition of  $H_2$  to  $H_2CO$  and has  $C_s$  symmetry. The remaining transition structures 9 and 10 correspond to the carbene-type insertions (reactions 5 and 6); both are without symmetry (point group  $C_1$ ).

As noted by DeFrees et al.,<sup>7</sup> single determinant (HF) calculations on the equilibrium geometries of molecules of this type are generally quite accurate. Typically correlation effects result in an increase of 0.01-0.03 Å in bond lengths. For transition structures, the effects of correlation

TABLE II: Calculated RHF and RMP2 (6-31G\*) Transition Structures<sup>a</sup>

structure	geometry RHF/6-31G* (RMP2/6-31G*)
5. 	$R_{CO} = 1.134$ (1.180), $R_{CH_a} = 1.094$ (1.092), $R_{CH_b} = 1.739$ (1.726), $R_{HH} = 1.328$ (1.356), $MCO \angle = 133.6$ (131.9), $H_aMC \angle = 57.8$ (58.9)
6. 	$R_{CO} = 1.270$ (1.322), $R_{CH_a} = 1.095$ (1.111), $R_{CH_b} = 1.219$ (1.276), $R_{OH_b} = 1.175$ (1.158), $H_bCO \angle = 56.3$ (52.9), $H_aCO \angle = 115.9$ (112.9)
7. 	$R_{CO} = 1.347$ (1.360), $R_{CH_a} = 1.109$ (1.127), $R_{OH_b} = 0.951$ (0.971), $H_aCO \angle = 104.9$ (104.2), $H_bOC \angle = 115.2$ (117.4), $H_aCOH_b \angle = 90.1$ (90.8)
8. 	$R_{CO} = 1.310$ (1.330), $R_{CH_a} = R_{CH_b} = 1.087$ (1.102), $R_{CH_c} = 1.408$ (1.430), $R_{CH_d} = 1.299$ (1.255), $R_{OH_d} = 1.385$ (1.424), $R_{H_cH_d} = 0.947$ (0.982), $H_aCH_b \angle = 112.9$ (111.8), $H_{ab}CO \angle = 154.4$ (153.0), $CM'M' \angle = 66.4$ (62.5), $M'M'H_d \angle = 54.7$ (50.9)
9. 	$R_{CO} = 1.347$ (1.351), $R_{CH_a} = 1.084$ (1.100), $R_{OH_b} = 0.947$ (0.973), $R_{CH_c} = 1.574$ (1.760), $R_{CH_d} = 1.298$ (1.311), $R_{H_cH_d} = 0.852$ (0.879), $H_aCO \angle = 109.1$ (106.6), $H_bOC \angle = 108.6$ (107.2), $H_aCH_c \angle = 83.4$ (81.9), $H_aCH_d \angle = 106.6$ (103.8), $H_cCH_d \angle = 32.7$ (28.8), $H_cCO \angle = 101.4$ (104.6), $H_dCO \angle = 113.8$ (114.9), $H_aCOH_b \angle = 162.9$ (172.5)
10. 	$R_{CO} = 1.806$ , $R_{CH_b} = 1.308$ , $R_{CM} = 1.475$ , $R_{OH_a} = 0.951$ , $R_{OH_b} = 1.116$ , $R_{CH_c} = 1.080$ , $R_{CH_d} = 1.077$ , $H_aOH_b \angle = 107.0$ , $H_cCH_d \angle = 110.8$ , $CMH_b \angle = 61.9$ , $H_cCM \angle = 108.3$ , $H_dCM \angle = 108.3$ , $H_bMC \angle = 98.1^\circ$

<sup>a</sup> M is used to denote bond midpoints.

TABLE III: Effects of Correlation on Selected Bond Lengths,  $\Delta R_{ab} = R_{ab}(\text{RMP2}) - R_{ab}(\text{RHF})$ 

reaction	bond	$\Delta R_{ab}, \text{\AA}$		
		reactant	product	transition structure
$H_2 + CO \rightarrow H_2CO$	C-O	0.038	0.036	0.046
	H-H	0.008	0.040	0.028
$H_2CO \rightarrow HCOH$ (trans)	C-O	0.036	0.023	0.052
$HCOH$ (trans) $\rightarrow$ $HCOH$ (cis)	C-O	0.023	0.019	0.013
$H_2 + H_2CO \rightarrow H_3COH$	C-O	0.036	0.024	0.020
	H-H	0.008		0.035
$H_2 + HCOH \rightarrow H_3COH$	C-O	0.023	0.024	0.004
	H-H	0.008	0.017	0.027
	C-H	0.014	0.009	0.016
	O-H	0.027	0.024	0.026

are found to be slightly larger although similar in trends to those found for the equilibrium structures. For example, correlation effects increase the C-O bond lengths of carbon monoxide and formaldehyde by 0.038 and 0.036 Å, respectively. For comparison correlation increases the C-O bond length of the transition structure connecting formaldehyde and carbon monoxide by 0.046 Å. Other exam-

TABLE IV: 6-31G\*\* Total Energies (hartrees) Based on RHF/6-31G\* Geometries

species	RHF	RMP2	RMP3	RMP4
H <sub>2</sub>	-1.131 33	-1.157 65	-1.163 14	-1.164 54
H <sub>2</sub> O	-76.023 57	-76.219 35	-76.225 82	-76.228 10
CH <sub>2</sub> ( <sup>1</sup> A <sub>1</sub> )	-38.876 30	-38.987 05	-39.006 09	-39.010 04
CO	-112.737 88	-113.018 04	-113.017 32	-113.027 31
HCOH (cis)	-113.782 74	-114.080 24	-114.093 99	-114.101 36
HCOH (trans)	-113.791 49	-114.088 73	-114.102 27	-114.109 58
H <sub>2</sub> CO	-113.869 74	-114.181 18	-114.188 77	-114.196 31
H <sub>3</sub> COH (stag.)	-115.046 68	-115.381 28	-115.399 08	-115.403 77
H <sub>2</sub> C··OH <sub>2</sub>	-114.912 89	-115.230 20	-115.252 67	-115.260 21
H <sub>2</sub> C··HOH	-114.908 91	-115.216 91	-115.241 93	-115.247 82
H <sub>2</sub> + CO ↔ H <sub>2</sub> CO <sup>a</sup>	-113.702 41	-114.027 98	-114.032 27	-114.044 14
H <sub>2</sub> CO ↔ HCOH <sup>a</sup>	-113.709 31	-114.038 33	-114.039 56	-114.051 24
HCOH (cis) ↔ HCOH (trans) <sup>a</sup>	-113.747 29	-114.037 30	-114.053 16	-114.060 01
H <sub>2</sub> + H <sub>2</sub> CO ↔ H <sub>3</sub> COH <sup>a</sup>	-114.869 21	-115.220 06	-115.231 42	-115.239 59
H <sub>2</sub> + HCOH (trans) ↔ H <sub>3</sub> COH <sup>a</sup>	-114.885 04	-115.226 17	-115.244 10	-115.250 82
CH <sub>2</sub> + H <sub>2</sub> O ↔ CH <sub>3</sub> OH <sup>a</sup>	-114.890 05	-115.238 12	-115.251 92	-115.260 39

<sup>a</sup> Transition structure.

TABLE V: 6-31G\*\* Total Energies (hartrees) Based on RMP2/6-31G\* Geometries

species	RMP2	RMP3	RMP4(SDQ)
H <sub>2</sub>	-1.157 65	-1.163 16	-1.164 57
H <sub>2</sub> O	-76.219 65	-76.225 87	-76.228 32
CH <sub>2</sub> ( <sup>1</sup> A <sub>1</sub> )	-38.987 16	-39.006 30	-39.010 30
CO	-113.021 22	-113.017 82	-113.029 86
HCOH (cis)	-114.081 00	-114.094 26	-114.102 14
HCOH (trans)	-114.089 69	-114.102 67	-114.110 54
H <sub>2</sub> CO	-114.183 48	-114.189 69	-114.198 17
H <sub>3</sub> COH (stag.)	-115.381 91	-115.399 39	-115.404 33
H <sub>2</sub> C··OH <sub>2</sub>	-115.235 60	-115.255 10	-115.262 05
H <sub>2</sub> C··HOH	-115.217 53	-115.242 24	-115.248 29
H <sub>2</sub> + CO ↔ H <sub>2</sub> CO	-114.031 71	-114.034 17	-114.047 95
H <sub>2</sub> CO ↔ HCOH <sup>a</sup>	-114.039 89	-114.040 36	-114.053 58
H <sub>2</sub> + H <sub>2</sub> CO ↔ H <sub>3</sub> COH <sup>a</sup>	-115.221 73	-115.232 05	-115.240 99
HCOH (cis) ↔ HCOH (trans) <sup>a</sup>	-114.037 76	-114.053 40	-114.060 50
H <sub>2</sub> + HCOH ↔ H <sub>3</sub> COH <sup>a</sup>	-115.225 60	-115.243 24	-115.251 14

<sup>a</sup> Transition structure.

TABLE VI: Relative Energies (kcal/mol) from RMPn/6-31G\*\* Calculations Based on RHF/6-31G\* Geometries

	RHF	RMP2	RMP3	RMP4
2H <sub>2</sub> + CO	0.0	0.0	0.0	0.0
H <sub>2</sub> + H <sub>2</sub> CO	-0.3	-3.4	-5.2	-2.8
H <sub>3</sub> COH	-29.0	-30.1	-34.8	-29.7
H <sub>2</sub> + HCOH (cis)	54.3	59.9	54.3	56.8
H <sub>2</sub> + HCOH (trans)	48.8	54.6	49.1	51.6
H <sub>2</sub> O··CH <sub>2</sub>	55.0	64.7	57.1	60.4
HOH··CH <sub>2</sub>	57.5	73.1	63.8	68.1
H <sub>2</sub> O + CH <sub>2</sub> ( <sup>1</sup> A <sub>1</sub> )	63.2	79.7	70.1	74.2
2H <sub>2</sub> + CO ↔ H <sub>2</sub> + H <sub>2</sub> CO <sup>a</sup>	104.7	92.7	93.0	92.7
H <sub>2</sub> + H <sub>2</sub> CO ↔ H <sub>2</sub> + HCOH (trans) <sup>a</sup>	100.3	86.2	88.4	88.2
H <sub>2</sub> + HCOH (trans) ↔ H <sub>2</sub> + HCOH (cis) <sup>a</sup>	76.5	86.8	79.9	82.7
H <sub>2</sub> + H <sub>2</sub> CO ↔ H <sub>3</sub> COH <sup>a</sup>	82.4	71.1	70.4	73.3
H <sub>2</sub> + HCOH (trans) ↔ H <sub>3</sub> COH <sup>a</sup>	72.5	67.2	62.4	66.2
CH <sub>2</sub> + H <sub>2</sub> O ↔ H <sub>3</sub> COH <sup>a</sup>	69.3	59.7	57.5	60.2

<sup>a</sup> Transition structure. Note that the energies are relative to 2H<sub>2</sub> + CO.

ples of the effect of correlation on geometric parameters are summarized in Table III. From these results we see that, in some reactions, the transition structure C-O bond length is more affected by correlation than either the reactants or the products while in other reactions the reverse is true. Larger bond length correlation effects are found for those bonds which contribute significantly to the reaction coordinate. For example, in the H<sub>2</sub> + HCOH addition, correlation effects increase the two C-H "bond" lengths by 0.013 and 0.184 Å, where the total "bond" lengths are 1.311 and 1.760 Å, respectively. Similarly the H-H distance increases from an RHF value of 1.378 Å to an RMP2 result of 1.488 Å, a net increase of 0.110 Å.

Perhaps more important than the actual correlation-induced changes in geometry is the effect of these changes

on the total and relative energies of the species. Total energies are given in Tables IV and V. A comparison of the relative energies tabulated in Table VI, based on RHF geometries, to those of Table VII, based on RMP2 geometries, shows clearly that the correlation-induced geometry differences lead to only minor differences in the relative energies of these species. Typically the difference in relative energies here is less than 1 kcal/mol. For comparison, the total RMP2 energies of these species drop by 3-4 kcal/mol on going from the RHF geometry to the RMP2 geometry. Apparently then the only large differences between the RHF and RMP2 geometries are in the reaction coordinate parameters of transition structures which correspond to partially broken bonds with small force constants (Table VI). The fortuitous result is that, al-

TABLE VII: Relative Energies (kcal/mol) from RMP/6-31G\*\* Calculations Based on RMP2/6-31G\* Geometries

	RMP2	RMP3	RMP4	RMP4 (with zero-point correction) <sup>a</sup>
2H <sub>2</sub> + CO	0.0	0.0	0.0	0.0
H <sub>2</sub> + H <sub>2</sub> CO	-2.9	-5.4	-2.3	5.9
H <sub>3</sub> COH	-28.5	-34.7	-28.4	-10.5
H <sub>2</sub> + HCOH (cis)	61.4	54.4	57.9	65.5
H <sub>2</sub> + HCOH (trans)	56.0	49.1	52.6	60.6
H <sub>2</sub> O...CH <sub>2</sub>	63.3	55.9	60.8	74.1
HOH...CH <sub>2</sub>	74.7	63.9	69.5	80.7
CH <sub>2</sub> ( <sup>1</sup> A <sub>1</sub> ) + H <sub>2</sub> O	81.4	70.3	75.5	84.4
2H <sub>2</sub> + CO ↔ H <sub>2</sub> + H <sub>2</sub> CO <sup>b</sup>	92.3	92.1	91.9	93.9
H <sub>2</sub> + H <sub>2</sub> CO ↔ H <sub>2</sub> + HCOH (trans) <sup>b</sup>	87.2	88.2	88.4	92.1
H <sub>2</sub> + HCOH (trans) ↔ H <sub>2</sub> + HCOH (cis) <sup>b</sup>	88.5	80.1	84.0	89.2
H <sub>2</sub> + H <sub>2</sub> CO ↔ H <sub>3</sub> COH <sup>b</sup>	72.0	70.3	74.1	86.0
H <sub>2</sub> + HCOH (trans) ↔ H <sub>3</sub> COH <sup>b</sup>	69.6	63.3	67.7	79.7

<sup>a</sup> Using the RHF/6-31G\* vibrational frequencies listed in Table VI. <sup>b</sup> Transition structure. Note that the energies are relative to 2H<sub>2</sub> + CO.

TABLE VIII: RHF/6-31G\* Vibrational Frequencies (cm<sup>-1</sup>) and Zero-Point Energies (kcal/mol)

molecule	frequencies	zero point
H <sub>2</sub>	4643(σ <sub>g</sub> )	6.6
CO	2439(σ)	3.5
H <sub>2</sub> CO	3233(b <sub>2</sub> ), 3161(a <sub>1</sub> ), 2030(a <sub>1</sub> ), 1680(a <sub>1</sub> ), 1383(b <sub>2</sub> ), 1336(b <sub>2</sub> )	18.3
H <sub>3</sub> COH	4118(a'), 3305(a'), 3232(a''), 3186(a'), 1664(a'), 1652(a''), 1637(a'), 1508(a'), 1289(a''), 1188(a'), 1164(a'), 348(a'')	34.7
HCOH (cis)	3985(a'), 2992(a'), 1611(a'), 1450(a'), 1370(a'), 1041(a'')	17.8
HCOH (trans)	4045(a'), 3101(a'), 1647(a'), 1446(a'), 1333(a'), 1128(a'')	18.2
H <sub>2</sub> O...CH <sub>2</sub>	4173(a''), 4067(a'), 3214(a'), 3151(a'), 1837(a'), 1572(a'), 1032(a'), 846(a'), 498(a'), 475(a''), 216(a'), 74(a'')	30.1
HOH...CH <sub>2</sub>	4150(a'), 3985(a'), 3235(a'), 3167(a'), 1859(a'), 1560(a'), 691(a''), 370(a'), 212(a''), 166(a'), 137(a'), 67(a'')	28.0
CH <sub>2</sub>	3193(b <sub>2</sub> ), 3130(a <sub>1</sub> ), 1564(a <sub>1</sub> )	11.3
H <sub>2</sub> O	4190(b <sub>2</sub> ), 4072(a <sub>1</sub> ), 1826(a <sub>1</sub> )	14.4
transition structures <sup>a</sup>		
H <sub>2</sub> + CO ↔ H <sub>2</sub> CO	3263(a'), 2149(a'), 1306(a'), 1056(a''), 755(a'), 2184i(a')	12.2
H <sub>2</sub> CO ↔ HCOH (trans)	3168(a'), 2816(a'), 1649(a'), 1431(a'), 649(a''), 2710i(a')	13.9
HCOH (t) ↔ HCOH (cis)	4070, 2977, 1524, 1281, 890, 1364i	15.4
H <sub>2</sub> + H <sub>2</sub> CO ↔ H <sub>3</sub> COH	3278(a''), 3209(a''), 2320(a'), 2053(a'), 1657(a'), 1626(a'), 1361(a'), 1350(a''), 1280(a''), 1048(a''), 886(a'), 2554i(a')	28.7
H <sub>2</sub> + HCOH (trans) ↔ H <sub>3</sub> COH	4097, 3285, 2873, 1829, 1564, 1445, 1279, 1160, 1156, 834, 608, 1427i	28.8
CH <sub>2</sub> + H <sub>2</sub> O ↔ CH <sub>3</sub> OH	4088, 3395, 3296, 2413, 1613, 1555, 1256, 1103, 868, 575, 529, 1712i	29.6

<sup>a</sup> For each of the transition structures, the last frequency is the imaginary reaction coordinate frequency.

TABLE IX: Comparison of RMP and CI Activation Energies

reaction	activation energy, kcal/mol					
	RHF	RMP2	RMP3	RMP4	CI-(1 + 2) <sup>a</sup>	CI-(1 + 2) + QC <sup>b</sup>
H <sub>2</sub> CO → H <sub>2</sub> + CO	105.0	96.1	98.2	95.5	97.3	93.6
H <sub>2</sub> CO → HCOH (trans)	100.6	89.6	93.6	91.0	91.8	88.8
HCOH (trans) → HCOH (cis)	27.7	32.2	30.8	31.1	27.4 <sup>c</sup>	27.5 <sup>c</sup>

<sup>a</sup> DZ + POL singles and doubles CI results from ref 9. <sup>b</sup> DZ + POL singles and doubles CI with quadruple correction from ref 9. <sup>c</sup> DZ results (no polarization functions).

though the geometry changes are quite large, they are energetically insignificant. Thus we conclude that for reactions of the type considered here, the use of RHF geometries can be expected to introduce errors of only ~1 kcal/mol in the relative energies of the structures. A similar conclusion was reported by GS on the basis of limited reoptimization at the DZ-CI level.

*The H<sub>2</sub>CO Species.* In this work we have considered four minimum energy structures on the H<sub>2</sub>CO potential surface and the three transition structures connecting these minima. As these features of the potential energy surface have already been well characterized in the extensive CI calculations of GS,<sup>9</sup> the main purpose here will be to compare the RMP results to those of the CI method. In

the following discussion then we emphasize the results obtained by using RHF geometries in order to facilitate comparison with the GS results. As noted in the previous section, the relative energies based on RMP2 geometries are not greatly different from those based on RHF geometries.

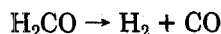
The relative energies for RHF/6-31G\*\* calculations reported here agree very well (to within 0.7 kcal) with those reported by GS with a comparable (DZ plus POL) basis set. At these geometries the RMP4 calculations generally lead to relative energies that lie between the singles plus doubles CI results and those with an added correction for the effect of unlinked cluster quadrupole excitations (using the Davidson formula),<sup>20</sup> suggesting that the correction

formula overestimates the importance of these terms.

The complete set of calculated harmonic frequencies (RHF/6-31G\*) is listed in Table VIII. For the most part, these are in moderate accord with those obtained for the H<sub>2</sub>CO stationary points by GS using a double-zeta (DZ) basis. For formaldehyde, they obtained 3364(b<sub>2</sub>), 3234(a<sub>1</sub>), 2123(a<sub>1</sub>), 1435(a<sub>1</sub>), 1332(b<sub>2</sub>), 1320(b<sub>1</sub>). The principal difference is for the lowest a<sub>1</sub> frequency (HCO bend) for which we obtain a large value of 1680. The experimental (anharmonic) frequencies are<sup>27</sup> 2843(b<sub>2</sub>), 2783(a<sub>1</sub>), 1746(a<sub>1</sub>), 1500(a<sub>1</sub>), 1249(b<sub>2</sub>), and 1167(b<sub>1</sub>). Compared with these observed values, all the calculated frequencies are too large, usually by 10–15%, a common experience with Hartree–Fock theory. A portion of this discrepancy arises from the fact that the theoretical frequencies refer to strictly harmonic vibrations. For formaldehyde, experimental estimates for the harmonic frequencies are available,<sup>27</sup> 3009(b<sub>2</sub>), 2944(a<sub>1</sub>), 1764(a<sub>1</sub>), 1563(a<sub>1</sub>), 1288(b<sub>2</sub>), and 1191(b<sub>1</sub>). This improves the agreement between theory and experiment. For the transition structure formaldehyde ↔ *trans*-hydroxycarbene, a major deviation between our results and GS is found. We obtain only 649 cm<sup>-1</sup> for the out-of-plane (a'') frequency compared with their value of 4323.<sup>21</sup>

The theoretical harmonic frequencies have been used to compute zero-point vibrational energies, which are also listed in Table VIII. The imaginary frequencies for the transition structures are omitted in these calculations. The final column of Table VII gives a set of relative energies in which the MP4(SDQ) values have been corrected for the zero-point vibrations.

The vibrationally corrected energies in Table VII may be compared directly with differences of experimental heats of formation at 0 K. For the exothermic hydrogen elimination reaction



the theory gives a reaction energy of -5.9 kcal/mol. Experimentally the energy is only -2.1 kcal/mol.<sup>25</sup> Part of this discrepancy can be traced to over-estimation of zero-point vibrational corrections. If we use experimental frequencies for H<sub>2</sub>, CO, and H<sub>2</sub>CO in combination with MP4(SDQ) energies, the energy is reduced to -4.5 kcal/mol. However, a difference of 2.4 kcal/mol remains; it is not clear at present whether this is due to a basis set deficiency or to inadequate computation of correlation energy corrections.

For the singlet hydroxycarbene HCOH, our results show that the *trans* form lies 54.7 kcal/mol above formaldehyde after correction for zero-point vibrations; the *cis* form is 4.9 kcal/mol higher still. The rotational barrier in HCOH is 28.6 kcal/mol (from the *trans* form). All of these values are very close to the corresponding numbers obtained by GS.

Again using the calculated RHF zero-point energies from Table VIII to correct the RMP4 energies, we obtain the following activation energies: H<sub>2</sub>CO → H<sub>2</sub> + CO, *E*<sub>a</sub> = 89.3 kcal/mol; H<sub>2</sub>CO → HCOH (*trans*), *E*<sub>a</sub> = 86.6 kcal/mol. Thus we conclude that the path leading to *trans*-hydroxycarbene is available at a lower energy than that for molecular dissociation of formaldehyde to H<sub>2</sub> + CO. This may be related to experiments interpreted to support the intermediacy of HCOH in the low-temperature matrix photochemistry of formaldehyde<sup>22</sup> and to the studies of Houston and Moore,<sup>11</sup> who said that at a low pressure, the rate of disappearance of H<sub>2</sub>CO (in photolysis) is much greater than the rate of appearance of CO, indicating the presence of a long-lived intermediate. It is important to note that at low pressure, formation of hydroxycarbene is

a reversible process with an equilibrium constant strongly favoring formaldehyde. At higher pressures, however, bimolecular processes for removal of hydroxycarbene become feasible because of the extremely reactive nature of this species. This would result in an increase in the rate of disappearance of formaldehyde at higher pressures.

These results differ from those of GS in the predicted energetic ordering of the molecular dissociation and 1,2 hydrogen migration transition structures. This is primarily due to the high out-of-plane vibration frequency they use for the latter.

With regard to the "width" of the barriers, as characterized by the imaginary (reaction coordinates) vibrational frequencies, the present results (Table VIII) are in reasonable agreement with the GS study. For the dissociation and rearrangement transition structures GS obtain imaginary frequencies of 2692 and 2705 cm<sup>-1</sup> while the RHF/6-31G\* frequencies are 2184 and 2710 cm<sup>-1</sup>, respectively. Thus the present calculations indicate a larger difference in the "widths" of the barriers associated with the two decomposition pathways.

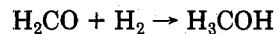
One possibility suggested by the calculated activation energies is the existence of a direct 1,2-elimination pathway from *cis*-hydroxymethylene to carbon monoxide. A saddle point corresponding to this elimination was located. However, the energy (relative to H<sub>2</sub>CO) of this saddle point is calculated to be 114 kcal/mol, well above that of the 1,1-elimination route. We conclude that, at moderate temperatures, this pathway will not compete with 1,1 elimination.

At this point we should note that there is a third pathway for destruction of formaldehyde that has not been examined in these calculations, the radical dissociation process leading to atomic hydrogen and formyl radicals. Experimental estimates of the formaldehyde C–H bond energy are in the range of 85–89 kcal,<sup>14,15</sup> coinciding with the observed threshold for radical dissociation.<sup>13</sup> The most accurate calculations on the molecular dissociation and rearrangement processes (Table V) lead to 0 K activation energies in this same range (88.0 and 86.2 kcal, respectively). Experimentally it has been observed that at low energies, 80–85 kcal, the molecular dissociation process occurs but the radical dissociation does not.<sup>12</sup> The difference, then, between the calculated activation energy for molecular dissociation and the observed threshold can be attributed either to tunneling effects (as suggested by GS and supported by Miller<sup>16</sup>) or to errors in the calculated activation energies.

**The H<sub>4</sub>CO Species.** The three minimum energy H<sub>4</sub>CO structures considered here are two loose complexes of CH<sub>2</sub>(<sup>1</sup>A<sub>1</sub>) and H<sub>2</sub>O (3 and 4) and methanol. Of these, only the methanol structure has been previously reported. Relative energies are listed in Tables VI and VII.

The RHF harmonic frequencies of methanol (Table VIII) may be compared with the full set of experimental frequencies. Experimental values<sup>28</sup> are 3681(a'), 3000(a'), 2960(a''), 2844(a'), 1477(a'), 1477(a''), 1455(a'), 1345(a'), 1165(a''), 1060(a'), 1033(a'), 295(a''). As with formaldehyde, all of these frequencies are around 10–15% too high; however, corrections for the anharmonicity of the experimental values would improve this agreement.<sup>29</sup>

The energy of the exothermic hydrogenation reaction



can be compared with experimental data. Using values of -25.1 and -48.0 kcal/mol for 0 K heats of formation of formaldehyde and methanol, respectively, the experimental reaction energy is -22.9 kcal/mol. The theoretical value (corrected for zero-point vibrations) is -16.4 kcal/mol. If



experimental vibration frequencies are used, the corresponding value is  $-17.4$  kcal/mol.

In complex 3, methylene acts as a Lewis acid, accepting electron density through delocalization of the oxygen lone pair into the unoccupied methylene  $p-\pi$  orbital. In complex 4 the acid-base roles are reversed, methylene now acting as a Lewis base and donating electron density through the interaction of the methylene lone pair with the adjacent hydroxyl hydrogen. In both complexes the resulting binding is quite weak, 14.7 and 6.0 kcal/mol, respectively in the most accurate calculations (RMP4/6-31G\*\*//RMP2/6-31G\*). Zero-point effects decrease these binding energies to 10.3 and 3.7 kcal/mol, respectively. The detailed structures and energies of 3 and 4 are summarized in Tables I, VI, and VII. A third minimum energy structure, corresponding to a rotation of  $\sim 100^\circ$  about the C-O bond of 3, was also located. This is calculated to lie  $\sim 2$  kcal/mol above 3 presumably due both to steric interactions between the hydrogens and to the interaction of the  $\text{CH}_2$  and  $\text{H}_2\text{O}$  dipoles. It is interesting to note that the 10.3 kcal/mol binding of  $\text{H}_2\text{C}\cdots\text{OH}_2$  is close to current estimates of the singlet-triplet separation in methylene itself. Hence stability of the complex with respect to dissociation into water and triplet methylene is probably small.

Three transition structures corresponding to reactions 4-6 were also examined. First consider the transition structure corresponding to hydrogenation of formaldehyde, 8. Although symmetry allowed, this addition is formally  $2\text{S} + 2\text{S}$  and is therefore expected to involve a relatively high activation energy. The actual calculated activation energy for this process is 76 kcal/mol (zero-point effects increase this to 80 kcal/mol). Although quite high this activation energy is below any of the bond energies in the  $\text{H}_2 + \text{H}_2\text{CO}$  system and thus is expected to be the most favorable pathway for hydrogenation. The transition structure shows the  $\text{H}_2$  approach is slightly skewed toward the carbon end of the double bond. In molecular orbital terminology this can be accounted for by considering the interaction of the  $\text{H}_2$  bond orbital with the lowest unoccupied MO of formaldehyde, the  $\pi^*$  orbital. Since the  $\pi$  bond of formaldehyde is shifted toward the oxygen, the  $\pi^*$  is necessarily shifted toward the carbon leading to a transition state skewed toward the carbon.

This addition is significantly exothermic (calculated exothermicity  $-26.1$  kcal/mol, observed  $-33.6$ ), and therefore Hammond's postulate predicts a reactant-like transition structure. This prediction is only partially supported by the calculations. For example, while the approaching  $\text{H}_2$  bond is not greatly extended ( $\sim 0.2$  Å longer than is the reactant), the C-O bond of the transition structure (1.330 Å) is approximately halfway between that of formaldehyde (1.220 Å) and methanol (1.423 Å). This latter result can also be understood by considering the interaction of the  $\text{H}_2$  bond pair with the formaldehyde  $\pi^*$  orbital. This  $\text{H}_2$ -to- $\pi^*$  shift would naturally lead to an increased C-O bond length, as observed.

It is interesting to note that the 1,2 hydrogenation of formaldehyde is much more facile than the 1,2 hydrogenation of CO. As noted in the previous section, the saddle point for the latter process is 114 kcal/mol above the reactants while in the former the activation energy is only 76 kcal/mol. This is undoubtedly a reflection of both the overall energetics (the formaldehyde hydrogenation is  $\sim 30$  kcal/mol exothermic while the carbon monoxide 1,2 hydrogenation is 58 kcal/mol endothermic) and the higher-lying  $\pi^*$  orbital of carbon monoxide (due to the shorter C-O bond length).

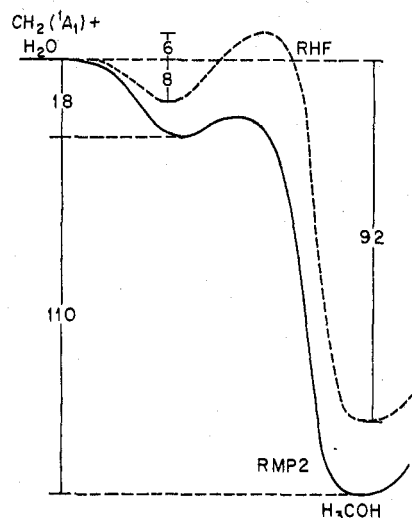


Figure 1. Schematic comparison of RHF and RMP2 reaction profiles for the addition of  $\text{CH}_2(^1\text{A}_1)$  to  $\text{H}_2\text{O}$ . Energy differences are in kcal/mol.

Turning now to the 1,1 hydrogenation of hydroxycarbene (10), leading again to methanol, the theoretical transition structures and energetics are presented in Tables II, VI, and VII. The overall reaction is very exothermic ( $-84$  kcal) and on this basis is expected to have an "early" transition structure. The calculations support this qualitative conclusion, indicating for example an H-H distance in the transition structure of 0.88 Å, only 0.14 Å longer than that of  $\text{H}_2$ . This may be compared with the less exothermic formaldehyde hydrogenation in which the transition structure H-H bond is 0.98 or 0.24 Å longer than in  $\text{H}_2$ .

This hydrogenation is, in effect, a carbene insertion reaction. Earlier studies on the insertion of methylene into an H-H bond<sup>2,23</sup> led to the conclusion that there is virtually no activation energy for this process. It is interesting then to note that substitution by a hydroxy group drastically reduces the reactivity of the carbene toward insertions. The calculated activation energy here is 15.1 kcal (this is further increased by 4.0 kcal due to zero-point effects). This can be explained as a combination of a  $\sigma$ -withdrawing effect (stabilizing the carbene lone-pair orbital and thus reducing the reactivity) and a  $\pi$ -donating effect (partially occupying the carbene  $p-\pi$  orbital and thereby making interactions with an approaching  $\text{H}_2$  less favorable).

The final reaction considered is the addition of  $\text{CH}_2(^1\text{A}_1)$  and  $\text{H}_2\text{O}$  forming methanol, also a carbene insertion reaction. The RHF barrier to this insertion is 6 kcal; however the RMP energies at this RHF transition structure are all well below the RMP energies of  $\text{CH}_2 + \text{H}_2\text{O}$  (see Table III). A number of attempts were made to locate an RMP2 transition structure for this insertion with the conclusion that at the RMP2 level there is no significant barrier to the insertion. For insertion of singlet  $\text{CH}_2$  into  $\text{H}_2$ , no activation energy is found at either RHF or correlated level.<sup>2,28,24</sup>

Several attempts were made to locate transition structures connecting the two  $\text{CH}_2\text{-H}_2\text{O}$  complexes with methanol. However, because of the complexity of the potential surface in this region, these attempts were not successful. We estimate however that the barriers separating these complexes from methanol to be on the order of 2-3 kcal, making experimental detection of the complexes difficult. These results on the addition of singlet  $\text{CH}_2$  to  $\text{H}_2\text{O}$  are summarized schematically in Figure 1.

## Conclusions

First, with regard to the chemistry on the  $\text{H}_4\text{CO}$  po-

TABLE X: Comparison of 6-31G\*\*, 6-31G\*, 4-31G, and STO-3G Activation Energies (RMP4)

reaction	activation energies, kcal/mol			
	6-31G**	6-31G*	4-31G	STO-3G
H <sub>2</sub> CO → H <sub>2</sub> + CO	95.5	96.7	94.5	119.4
H <sub>2</sub> CO → HCOH	91.0	93.7	103.7	118.4
H <sub>2</sub> + H <sub>2</sub> CO → H <sub>3</sub> COH	76.1	83.7	93.9	146.1
H <sub>2</sub> + HCOH → H <sub>3</sub> COH	14.6	19.3	19.0	40.2

tential energy surface, the conclusions from the calculations reported here may be summarized as follows:

(1) The lowest energy pathway for the unimolecular destruction of formaldehyde is the 1,2 hydrogen shift forming hydroxycarbene. The calculated activation energy for this reversible process is 86.2 kcal/mol, placing it 1.8 kcal/mol below the competing irreversible molecular dissociation process leading to H<sub>2</sub> + CO.

(2) Of the three pathways considered for the unimolecular destruction of methanol, the lowest energy route leads to hydroxycarbene ( $E_a$  = 90.2 kcal/mol). At higher energies two other concerted pathways are accessible, one to methylene and H<sub>2</sub>O ( $E_a$  = 94.9 kcal/mol) and a second leading to formaldehyde and molecular hydrogen ( $E_a$  = 96.5 kcal/mol). Of these only the first is likely to lie below the lowest energy radical cleavage process leading to ·CH<sub>3</sub> + ·OH (the observed C–O bond energy is ~91.5 kcal/mol).

(3) There is little or no barrier to the insertion of singlet methylene into an OH bond of H<sub>2</sub>O.

(4) There is a significant barrier (19.1 kcal) to the insertion of hydroxycarbene into an H<sub>2</sub> bond. This is to be compared with earlier results which show no barrier for the insertion of singlet methylene into H<sub>2</sub>.

With regard to the theoretical methods used here, we conclude that RMP/6-31G\*\* calculations lead to a reasonably accurate (±5 kcal) model of the chemistry of this system, comparable to that of extensive CI calculations. Furthermore the use of RHF equilibrium and transition structures leads to only relatively small errors (~1 kcal) in relative energies.

**Acknowledgment.** This research was supported by the National Science Foundation (Grant CHE-79-01061).

## Appendix

The theoretical activation energies present in the preceding sections are all derived from calculations employing 6-31G\*\* basis sets. Although basis-set effects on the relative energies of minimum energy species have been quite well studied, relatively little is known about basis-set effects on theoretical activation energies. It is relevant then, at this point, to consider the effect of using smaller, less flexible basis sets as might be necessary in studies of more complicated reactions. In Table X a comparison is made of activation energies from 6-31G\*\*, 6-31G\*, 4-31G, and STO-3G calculations. In all cases (except the 6-31G\*\*

calculations) the geometries were optimized by using RHF wave functions and the specified basis. The final energies shown in Table X were then obtained with RMP4 calculations at the RHF geometries.

We find that neglect of hydrogen polarization functions leads to errors of up to 6 kcal/mol in the activation energies. Neglect of d polarization functions leads, in one case, to an additional 10 kcal error. Finally we note that all of the STO-3G activation energies are much too high; the errors here range from 24 to 70 kcal. In particular the STO-3G activation energy for formaldehyde hydrogenation is almost twice the 6-31G\*\* result.

## References and Notes

- (1) (a) National Science Foundation, National Needs Postdoctoral Fellow 1978–79. (b) Merck, Sharp and Dohme Research Laboratory, Rahway, NJ 07000.
- (2) C. W. Bauschlicher, Jr., K. Haber, H. F. Schaefer III, and C. F. Bender, *J. Am. Chem. Soc.*, **99**, 3610 (1977).
- (3) (a) J. H. Davis and W. A. Goddard III, *J. Am. Chem. Soc.*, **99**, 7111 (1977); (b) J. H. Davis, W. A. Goddard III, and L. B. Harding, *ibid.*, **99**, 2919 (1977); (c) L. B. Harding and W. A. Goddard III, *ibid.*, **99**, 4520 (1977).
- (4) J. A. Pople, R. Krishnan, H. B. Schlegel, and J. S. Binkley, *Int. J. Quantum Chem.*, **14**, 545 (1978).
- (5) J. A. Pople, J. S. Binkley, and R. Seeger, *Int. J. Quantum Chem., Symp.*, **10**, 1 (1976).
- (6) R. Krishnan and J. A. Pople, *Int. J. Quantum Chem.*, **14**, 91 (1978).
- (7) D. J. DeFrees, B. A. Levi, S. K. Pollack, W. J. Hehre, J. S. Binkley, and J. A. Pople, *J. Am. Chem. Soc.*, **101**, 4085 (1979).
- (8) (a) R. L. Jaffe, D. M. Hayes, and K. Morokuma, *J. Chem. Phys.*, **60**, 5108 (1974); (b) R. L. Jaffe and K. Morokuma, *ibid.*, **64**, 4881 (1976).
- (9) J. D. Goddard and H. F. Schaefer III, *J. Chem. Phys.*, **70**, 5117 (1979).
- (10) R. R. Lucchese and H. F. Schaefer III, *J. Am. Chem. Soc.*, **100**, 298 (1978).
- (11) P. L. Houston and C. B. Moore, *J. Chem. Phys.*, **65**, 757 (1976).
- (12) A. Horowitz and J. G. Calvert, *Int. J. Chem. Kinet.*, **10**, 713 (1978).
- (13) (a) J. H. Clark, C. B. Moore, and N. S. Nogau, *J. Chem. Phys.*, **68**, 1264 (1978); (b) J. P. Reilly, J. H. Clark, C. B. Moore, and G. C. Pimentel, *ibid.*, **69**, 4381 (1978).
- (14) R. Walsh and S. W. Benson, *J. Am. Chem. Soc.*, **88**, 4570 (1966).
- (15) P. Warneck, *Z. Naturforsch. A*, **26**, 2047 (1971); **29**, 350 (1974).
- (16) W. H. Miller, *J. Am. Chem. Soc.*, **101**, 6810 (1979).
- (17) J. A. Pople, R. Krishnan, H. B. Schlegel, and J. S. Binkley, *Int. J. Quantum Chem.*, **S13**, 225 (1979).
- (18) P. C. Hariharan and J. A. Pople, *Mol. Phys.*, **27**, 209 (1974).
- (19) J. S. Binkley, R. A. Whiteside, R. Krishnan, R. Seeger, H. B. Schlegel, D. J. DeFrees, and J. A. Pople, to be submitted to the Quantum Chemistry Program Exchange.
- (20) (a) S. R. Langhoff and E. R. Davidson, *Int. J. Quantum Chem.*, **8**, 61 (1979); (b) E. R. Davidson and D. W. Silver, *Chem. Phys. Lett.*, **52**, 403 (1978).
- (21) Dr. Schaefer has informed us that their revised calculations give a frequency close to 600 cm<sup>-1</sup>.
- (22) J. R. Sodeau and E. K. C. Lee, *Chem. Phys. Lett.*, **57**, 71 (1978).
- (23) H. B. Schlegel and J. A. Pople, to be submitted.
- (24) D. Jeziorek and B. Zurawski, *Int. J. Quantum Chem.*, **16**, 277 (1979).
- (25) This result is obtained by using  $\Delta H_f^\circ(298) (\text{CH}_2\text{O}) = -25.95 \pm 0.11$  kcal/mol, from ref 26, and  $\Delta H_f^\circ(0) - \Delta H_f^\circ(298) = 0.9$  kcal, from the JANAF tables. The remaining heats of formation also come from the JANAF tables.
- (26) R. A. Fletcher and G. Pilcher, *Trans. Faraday Soc.*, **66**, 794 (1970).
- (27) J. L. Duncan and P. D. Mallinson, *Chem. Phys. Lett.*, **23**, 597 (1973).
- (28) A. Serrallach, R. Meyer, and Hs. H. Gunthard, *J. Mol. Spectrosc.*, **52**, 94 (1974).
- (29) H. B. Schlegel, Ph.D. Thesis, Queen's University, 1975.